

## FEATURE ARTICLE

## Design strategies for fluorescent biodegradable polymeric biomaterials

Cite this: *J. Mater. Chem. B*, 2013, **1**, 132

Yi Zhang<sup>ab</sup> and Jian Yang<sup>\*c</sup>

The combination of biodegradable polymer and fluorescent imaging has resulted in an important area of polymeric biomaterials: biodegradable fluorescent polymers. Researchers have made significant efforts in developing versatile fluorescent biomaterials due to their promising applications in biological/biomedical labeling, tracking, monitoring, imaging, and diagnostics, especially in drug delivery, tissue engineering, and cancer imaging. Biodegradable fluorescent polymers can function not only as implant biomaterials but also as imaging probes. Currently, there are two major classes of biodegradable polymers, which are used as fluorescent materials. The first class is the combination of non-fluorescent biodegradable polymers and fluorescent agents such as organic dyes and quantum dots. Another class of polymers shows intrinsic photoluminescence as polymers by themselves carrying integral fluorescent chemical structures in or pendent to their polymer backbone, such as Green Fluorescent protein (GFP), and the recently developed biodegradable photoluminescent polymer (BPLP). Thus there is no need to conjugate or encapsulate additional fluorescent materials for the latter. In the present review, we will review the fluorescent biodegradable polymers with emphases on material fluorescence mechanism, design criteria for fluorescence, and their cutting-edge applications in biomedical engineering. We expect that this review will provide an insightful discussion on the fluorescent biomaterial design and lead to innovations for the next generation of fluorescent biomaterials and fluorescence-based biomedical technology.

Received 4th September 2012  
Accepted 5th October 2012

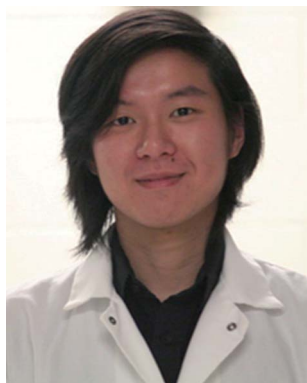
DOI: 10.1039/c2tb00071g

[www.rsc.org/MaterialsB](http://www.rsc.org/MaterialsB)

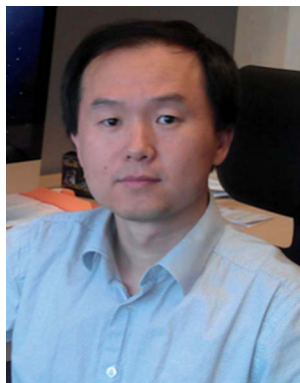
<sup>a</sup>Department of Bioengineering, University of Texas at Arlington, Arlington, TX 76010, USA

<sup>b</sup>Joint Biomedical Engineering Program, The University of Texas Southwestern Medical Center and The University of Texas at Arlington, Dallas, TX 75390, USA

<sup>c</sup>Department of Bioengineering, Materials Research Institute, The Huck Institutes of The Life Sciences, The Pennsylvania State University, W340 Millennium Science Complex, University Park, PA 16802, USA. E-mail: [jxy30@psu.edu](mailto:jxy30@psu.edu)



Dr Yi Zhang received his PhD from the Department of Bioengineering at the University of Texas at Arlington under the supervision of Dr Jian Yang. He has been working on the development of novel biodegradable polymers for tissue engineering, drug delivery and bioimaging applications.



Dr Jian Yang is an Associate Professor in the Department of Bioengineering at the Pennsylvania State University. Dr Yang directs a Transformative Biomaterials and Biotechnology Laboratory (TBBL) focusing on creating novel biomaterials based on the evolving understanding on the interactions of biomaterials and living organisms and developing transformative biotechnologies for applications in tissue engineering, drug delivery, medical device, and bioimaging. He has received an Early CAREER Award from the National Science Foundation (2010), and an Outstanding Young Faculty Member Award (2011) at the University of Texas, Arlington. He has published over 55 journal articles, and 12 issued or pending patents.

## 1 Introduction

Biomaterials are critical components of biomedical devices and products.<sup>1–5</sup> A novel biomaterial may create new fields of studies and opportunities to tackle unmet clinical problems. During the past few decades, biodegradable polymers have been central in biomaterial science for a wide variety of biomedical applications such as drug delivery, tissue engineering, and medical devices.<sup>3,6</sup> There are many types of biodegradable polymers such as polyesters, polyanhydrides, polyurethanes, poly(ester amides), and polyphosphazenes. Thereof, biodegradable polyesters are the most studied polymers, *e.g.*, polylactides, polyglycolides, and their copolymers, which are currently used in many food and drug administration (FDA) approved medical devices. Using biodegradable polymers as implant materials is beneficial as the implants may be degraded, absorbed, and cleared by the body once their missions are completed, leaving no foreign materials in the body. Among the above-mentioned biodegradable polymers, polyesters are the most attractive for many biomedical applications as these polymers mostly undergo degradation by hydrolysis in the body where water is ubiquitous, although the polymers may also possibly be degraded enzymatically.<sup>7</sup>

With careful molecular design, the physical properties of biodegradable polymers can be tailored into hard and stiff, soft and elastic, water soluble or insoluble, photo-crosslinkable or thermo-crosslinkable in order to meet the versatile needs of processing and use conditions in various applications.<sup>8–10</sup> On the other hand, fluorescent labeling and imaging have fueled the significant growth of life science and medical research due to the increasing demands on analyzing biomolecules, tracking biological processes, and visualizing diseases and therapeutic efficacy.<sup>11,12</sup> There has been an increasing interest in designing fluorescent biodegradable polymers to address some critical challenges in major biomedical applications such as those in tissue engineering and (cancer) drug delivery and imaging that are delineated below.

For tissue engineering, it has been somewhat disappointing that the expected success of tissue engineering still seems out of reach at this stage although the field of tissue engineering is evolving. Some fundamental understanding of the key elements of tissue engineering is still missing. For example, scaffold degradation *in vivo* is often predicted by the outcome of *in vitro* degradation studies.<sup>13</sup> However, the degradation rate of a biomaterial *in vitro* might not reflect its actual degradation rate *in vivo*. Quantitative determination of polymeric scaffold degradation *in vivo* has been problematic due to the difficulty of separating the infiltrated/regenerated tissues from the porous scaffolds. Although it is recognized that the scaffold degradation rate should match the rate of new tissue formation, biomaterial designs to control the *in vivo* scaffold degradation rate remain empirical due to the lack of *in vivo* quantitative validation. It is imperative to find an *in situ* real-time method to facilitate tracking or monitoring tissue regeneration and scaffold degradation processes without sacrificing animals. This issue has been rarely addressed previously. Thus, the field of tissue engineering remains a trial and error process, to some

degree. New measurement tools, engineering methods, design principles, non-invasive, and real-time assays are urgently needed to move the field of tissue engineering forward. To obtain *in situ* and real-time information on scaffold degradation and tissue infiltration/regeneration *in vivo* without traumatically explanting samples or sacrificing animals, it is essential that the biodegradable polymers can be used as non-invasive *in vivo* bioimaging probes, in addition to providing a suitable three-dimensional (3D) cell growth environment.

For drug delivery, it is well established that polymeric drug delivery systems can enhance efficacy and safety for cancer therapy by transporting chemotherapy agents directly to the tumor cells/tissues.<sup>14,15</sup> One of the major areas identified by the National Cancer Institute (NCI), in which nanotechnology may have a major impact on drug delivery, is “multifunctional therapeutics for combined diagnostic and therapeutic applications.” The National Institute of Health (NIH) also seeks proposals *via* The American Recovery and Reinvestment Act of 2009 Program to develop theranostic smart biomaterials for combined delivery of diagnostic and therapeutic agents for cancer management. All these national efforts in searching for novel cancer technologies point out a potential future breakthrough in cancer research: theranostic nano-biomaterials for cancer imaging and treatment. Theranostic nanomedicine intertwines drug delivery and diagnostic bioimaging, especially emphasizing on the use of non-invasive high-throughput imaging tools.<sup>16</sup> For cancer treatment, multifunctional polymeric nanoparticle systems are designed to simultaneously deliver therapeutic, targeting moieties, and imaging agents in a single setting.<sup>17,18</sup> For fluorescence imaging, polymeric nanoparticles are usually conjugated with additional organic dyes or quantum dots (QDs).<sup>19</sup> However, the poor photobleaching-resistance and low dye-to-particle conjugation ratios of organic dyes and the toxicity of QDs prevent their practical use *in vivo*. Since imaging agents themselves cannot be used as implants such as drug delivery carriers, the conjugation/encapsulation of imaging agents with drug delivery carriers is required to produce theranostic nanomaterials.<sup>20,21</sup> Unfortunately, encapsulating/conjugating imaging agents in/on nanoparticles may result in increased particle sizes, added complexity, and higher risk of adverse biological reactions. Such challenges might be resolved using biodegradable polymers, which themselves exhibit dual-functionality as drug delivery carriers and imaging probes.

Given the growing body of research in fluorescent biomaterial design and the critical needs in addressing some of the challenges in but not limited to tissue engineering and drug delivery, this review is aimed to emphasize on the design strategies for biodegradable fluorescent polymeric biomaterials. Key issues in the design criteria will be reviewed and discussed including material fluorescence mechanism, important fluorescence parameters such as excitation, emission, quantum yields, and extinction coefficient, and strategies to confer fluorescence to biodegradable polymers. The applications of biodegradable fluorescent polymers will also be reviewed. It is our hope that this review will serve as a guideline for anyone who is interested in innovating or using biodegradable fluorescent polymers for biomedical applications.

## 2 Fluorescence mechanism

Understanding the fluorescence mechanism of materials is a key in the design of biodegradable fluorescent polymers. Conventionally, the process of all the fluorescence is considered one-photon absorption (OPA). With the development of laser technology, various fluorescent materials have been designed or modified to be capable of undergoing the multi-photon absorption (MPA) process.<sup>22</sup> During the MPA process, the fluorophore simultaneously absorbs multiple photons to be raised into an excited state, and then emits a single photon at a certain wavelength. Since the energy to excite the fluorophore is provided by a sum of multiple photons, a photon with a lower energy state (longer wavelength) can be used for excitation. Therefore, MPA is capable of providing up-conversion fluorescence.<sup>23</sup> Due to the longer excitation wavelength and highly localized excitation, the fluorescence of MPA materials has a deeper penetration in tissue. Moreover, a longer excitation wavelength has a relatively lower phototoxicity,<sup>24</sup> thus it was considered that the MPA fluorophore is better for live cells/tissue than the OPA one. Besides, MPA confers many other promising effects, such as enhanced refractive-index changes of the medium, molecular dissociation or ionization, electron emission from the material's surface, induced conductivity in semiconductors, and induced polymerization.<sup>22</sup> Three structural components are essential for MPA materials: a strong  $\pi$ -electron donor, a polarizable  $\pi$ -bridge, and a strong  $\pi$ -electron acceptor.<sup>22</sup> The structural–property relationship has been well summarized in previous reviews.<sup>22,25</sup> Although MPA differs from conventional OPA, the fluorescent mechanism still remains the same.<sup>25</sup> Below we will review the fluorescence mechanism of the commonly used fluorescent materials.

Quantum dot (Qdot) is the major type of inorganic semiconducting fluorescent material. It not only includes cadmium selenide (CdSe) but also of many other semiconducting materials derived from the II and VI elemental groups (CdTe, CdS, CdHg, and ZnS) and III and V elemental groups (InAs, InP, and GaAs) of the periodic table.<sup>11</sup> The key word for their fluorescent mechanism is energy gap. All semiconductors have an energy band gap ( $E_g$ ) (Fig. 1a) between conduction band and valence band. When a photon is absorbed, the electron can be excited to the conduction band, and leave a hole on the valence band. Why do only Qdots have fluorescence while bulk semiconductors don't? This question leads us to another key word, quantum confinement. In the case of Qdots, the separation between excited electron and hole is smaller than their Bohr radius so that the exciton was squashed into a smaller space with more energy.<sup>26</sup> Therefore, the emission of Qdots is size dependent. The smaller the size, the more the energetic exciton and blue-shifting emission. In contrast, the bigger the size, the more the red-shifting emission. The tunable fluorescence of Qdots has been investigated for multicolor fluorescence imaging of cancer cells under *in vivo* conditions.<sup>27</sup> Since different compositions vary in energy gap, from 0.14 (HgTe) to 3.8 (ZnS),<sup>28,29</sup> the range of emission wavelength is different for different Qdots. For example, CdSe can emit from 470 nm to 670 nm, with a size change from 2 nm to 8 nm, whereas PbSe can emit from

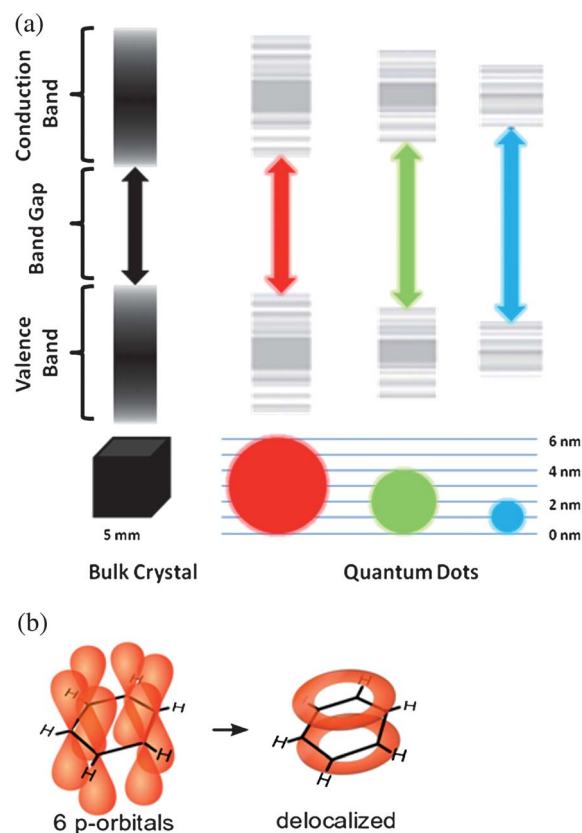


**Fig. 1** (a) Fluorescent mechanism of quantum dots. (b) Conjugated system of a benzene ring.

1120 nm to 1320 nm, with a size change from 3 nm to 4 nm. Generally, a small energy gap leads to a higher emission wavelength. Recently, quantum dots are capped with a shell of another semiconductor, mostly ZnS.<sup>30</sup> In the case of CdSe/ZnS core-shell particles, quantum yield was raised to 30–50% as compared to 5–15% of CdSe particles and the emission range was also moved to longer emission wavelengths.

Organic fluorescent materials include fluorescent polymer, small molecule dye, and green fluorescent protein. The widely accepted fluorescent mechanism is that the conjugated system results in fluorescence. According to the International Union of Pure and Applied Chemistry (IUPAC), conjugation is the overlap of one p-orbital with another across an intervening sigma bond. Therefore, organic compounds with alternating single and multiple bonds, normally an aromatic ring obeying Hückel's rule,<sup>31</sup> have a system of connected p-orbitals and allow a delocalization of  $\pi$  electrons across the system (Fig. 1b). The structure of some traditional small molecule dyes is listed in Fig. 2a. The energy gap of these materials is created by the conjugated  $\pi$ -system. The more extended the conjugation system, the more the red-shifting emission. Although small molecular organic dyes are totally different materials from Qdots, they have some drawbacks in common, such as cellular toxicity, and poor physical and chemical stability. Therefore, they both have been studied extensively to incorporate with biodegradable polymer for bioimaging application in order to function as implant materials or devices.

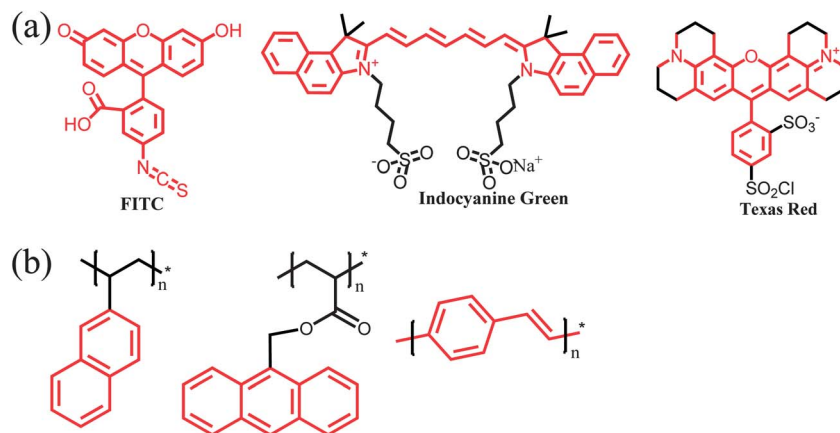


**Fig. 2** (a) Chemical structure of traditional small molecular dye (red represents the conjugated system). (b) Chemical structure of fluorescent polymers, poly(2-vinylnaphthalene), poly(9-anthracenylmethyl acrylate), and poly(*p*-phenylene vinylene) (from left to right) (red represents the conjugated system).

Fluorescent polymers can be divided into two classes. One is having a conjugated system pendent to the backbone (Fig. 2b). The other one is with the conjugated system along the backbone, like poly(*p*-phenylene vinylene) (Fig. 2b). The fluorescent mechanism is the same as for a small molecular dye. Recently, there is a new family of fluorescent dendrimers with the tetramine group, including poly(amido amine) (PAMAM), poly(propyleneimine) (PPI), and poly(ethyleneimine) (PEI). The first proposed fluorescent mechanism was the oxidation of hydroxyl end groups of PAMAM.<sup>32</sup> This hypothesis was later disproved by Imae's group that PPI and PEI with various end groups can emit blue fluorescence.<sup>33</sup> With more detailed studies, Imae and Chu<sup>34</sup> found that a more rigid, crowded structure of tertiary amines exhibits a higher fluorescence yield. Although the fluorescent mechanism still remains unclear, the tertiary amino on the dendritic backbone is speculated to be the key of fluorescence,<sup>34</sup> which is still under the rules of conjugation.

With the tremendously increased researches on Green Fluorescent Protein (GFP), the fluorescent mechanism of GFP has been revealed in decent detail. Although there are still some arguments, researchers have agreed on a cyclic ring fluorophore, *p*-hydroxybenzylideneimidazolinone.<sup>35</sup> With thorough studies on the primary, secondary, tertiary, and quaternary structure of GFP, it was found that the cyclic ring in GFP is composed of residues Ser or Thr65, Tyr66, and Gly67. Fig. 3a illustrates the currently accepted mechanism of the fluorophore formation. After a series of folding, cyclization, dehydration, and aerial oxidation,<sup>36</sup> the conjugated system is formed. As a natural organic compound, the fluorescent mechanism of GFP still obeys the conjugated system. Therefore, emission of GFP can also be tuned by extending the conjugation system (Fig. 3b). The task can be achieved by oligomerization and conjugating a more aromatic structure onto the fluorophore by a series of folding mutation. Gross *et al.*<sup>37</sup> have reported a red fluorescent protein "DsRed." The red fluorophore results from the autonomous multi-step post-translational modification of residues Gln66, Tyr67, and Gly68 into an imidazolidinone heterocycle with *p*-hydroxybenzylidene and acylimine substituents. Shaner *et al.*<sup>38,39</sup> have concluded monomeric fluorescent proteins that emit from yellow to red.

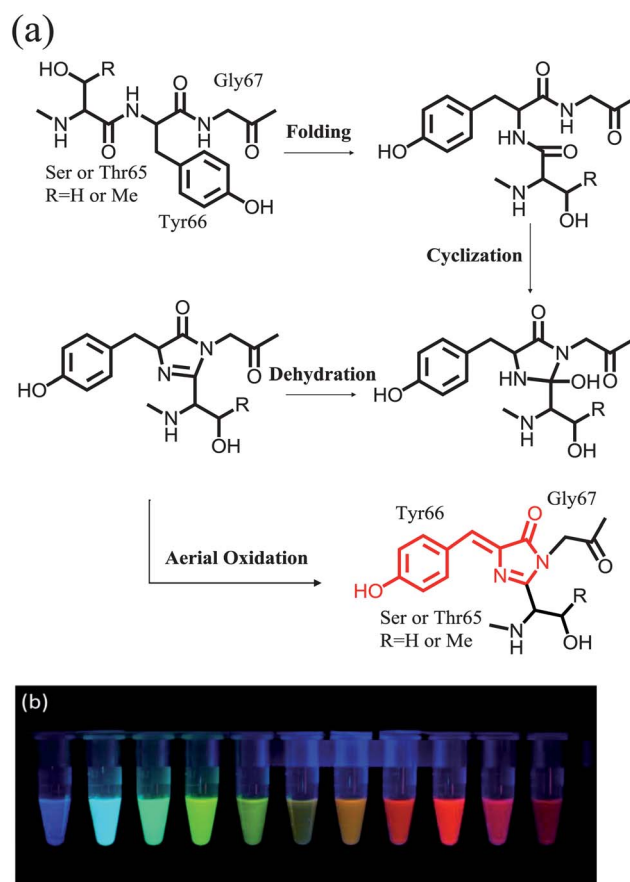


**Fig. 3** (a) The formation and final chemical structure of the fluorophore of GFP. (b) Different colors from various fluorescent proteins.<sup>111</sup>

By obeying the conventional rule of a conjugation system, fluorescence seems to be an irreconcilable conflict with biodegradability as water and fire. Therefore, there has not been any report of conventional fluorescent polymer being biodegradable. Recently, the authors' lab has developed a new type of biodegradable photoluminescent polymers (BPLPs) which possess an intriguing fluorescent mechanism although it is not

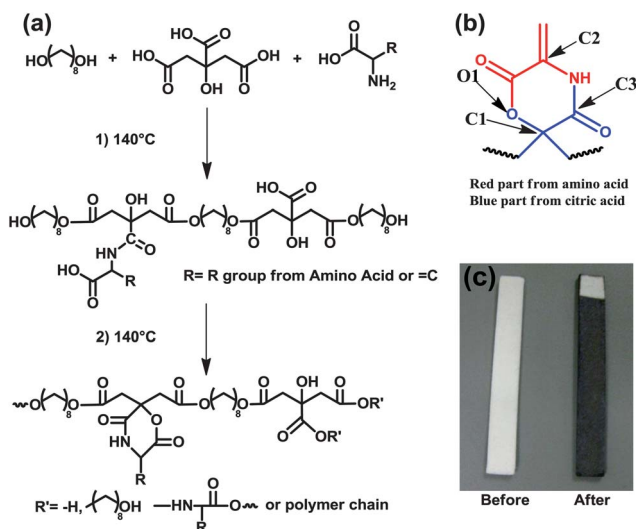


**Fig. 4** (a) Synthesis schematic of BPLPs, (b) chemical structure of six-member ring of BPLP-Cys and (c) test stripe turning black shows the release of hydrogen sulfide.

fully understood yet.<sup>40</sup> BPLPs were synthesized by reacting citric acid, aliphatic diol such as 1,8-octanediol, and α-amino acids through a convenient condensation reaction (Fig. 4a). Poly(octamethylene citrate) (POC) synthesized from only 1,8-octanediol and citric acid has very weak autofluorescence. Citric acid has been replaced with succinic acid and tricarboxylic acid for the synthesis, which turned out that neither of those polymers is fluorescent. A plausible hypothesis can be drawn from those simple reactions in that the side carboxylic and the germinal hydroxyl group from citric acid, together with an amino acid, results in fluorescence. All 20 essential α-amino acids have distinct fluorescence, including glycine which has no R groups. This further excludes the R group of the amino acid from the list of indispensables, as amidation and esterification are two possible reactions among amine, hydroxyl, and carboxyl groups. Considering the reacting rate and energy, the fastest reaction is between the amine and the side carboxyl group from citric acid. Based on the product of this amidation, we hypothesize a six-member ring structure (Fig. 4b) to be the fluorophore. The <sup>13</sup>C-NMR spectra of BPLP-cysteine provided evidence for the six-member ring structure.<sup>40</sup> For organic compounds, conjugation is the only known law of fluorescence. The basic requirement of a structure being conjugated is planarity. The hypothesized six-member ring has a similar structure as morpholine-2,5-dione. In the present case (Fig. 4b), hydrogen on C2 is substituted with an R-group, while hydrogens on C1 are substituted by polymer chains. Studies from other groups have proven the planarity of the ring, when hydrogens on C1 and C2 have been substituted.<sup>41</sup> In order to explain the conjugation of the whole ring structure, the theory of hyperconjugation needed to be introduced. This is a well-studied phenomenon, which was first defined by R. S. Mulliken in the late 1930s. It refers to the interaction of δ with an adjacent π-orbital. There is evidence showing that hyperconjugation not only extend the conjugation but also lead to fluorescence on its

own.<sup>42</sup> In the current six-member ring, the carbonyl group on C3 and the electronic pair from O1 both interact with a C–C δ bond on C1 to form hyperconjugation to explain the conjugation of a six-member ring. It is noteworthy that there is an outstanding red-edge effect (REE) on BPLP-serine (BPLP-Ser).<sup>40,43</sup> Previous studies have shown that fluorescence spectra can depend on excitation wavelength, when polar fluorophores are embedded into different rigid and highly viscous media.<sup>43</sup> The six-member ring structure of BPLPs is pendent on polymer chain, which can be considered as a rigid media. The excitation dependent emission of BPLP-Ser is a remarkable property, not only because it makes the fluorescence more controllable but also pushes it into the window of near infrared. This 6-member ring fluorophore hypothesis was further supported by the result that the use of β-amino acids can switch off the fluorescence due to the possible formation of a seven-member ring structure, which does not suffice the conjugation system as stated above.

### 3 Design criteria of fluorescent materials for biomedical application

To develop an ideal biodegradable fluorescent material for various bioimaging, the physiological, physicochemical, and photophysical properties should all be taken into consideration. For different bioimaging applications, a fluorophore should be chosen with careful consideration of its photophysical, physiological, and physicochemical property.

To better describe the photophysical property of a fluorescent material, there are several parameters to be understood. Firstly, excitation and emission, they determine the color of the fluorescence. As we discussed above, the emission of quantum dots is size dependent, while the one of organic compounds can be manipulated by chemical modification.<sup>27,38,44</sup> Considering the biomedical application, penetration depth in the biological tissue is important as well. Light with a longer wavelength has a longer penetration depth in tissues.<sup>44</sup> The brightness of fluorescence is the second consideration after fluorescence color. Precisely speaking, the brightness is determined by two parameters, extinction coefficient and quantum yield. The extinction coefficient stands for how many photons a substance can absorb under a given wavelength, which is excitation wavelength. Quantum yield shows the efficiency of a substance that emits light, specified at a given emission wavelength. In a common word, it represents how many photons can be emitted, when 100 of them are absorbed. In the comparison of the brightness of different fluorescent proteins, the product of molar extinction coefficient and quantum yield has been used.<sup>39</sup> Although each fluorophore has a fixed value of extinction coefficient and quantum yield at a given wavelength, those values can be varied with different factors such as solvent, temperature, and pH. The endurance of fluorescent materials to photobleaching is also a very important optical property. It is determined by the time to bleach from an initial emission rate of 1000 photons per s down to 500 photons per s.<sup>38,39</sup> In most cases, it stands for the photostability. Aggregation caused quenching (ACQ) of fluorescent materials should be taken into consideration when fluorophores are required at a high

**Table 1** Optical properties of different fluorescent materials (for quantum yield and extinction coefficient, samples were tested using water as solvent, unless specified)

Category	Fluorescent material	Emission (nm)	Quantum yield	Extinction coefficient ( $M^{-1} cm^{-1}$ )	$t_{1/2}$ for bleach (s)
Quantum dots	CdS	370–500	<0.60	100 000–950 000	
	CdSe	470–660	0.65–0.85	100 000–700 000	
	CdTe	520–750	0.30–0.75	130 000–600 000	
Organic dyes	FITC	541	0.97 (ethanol)	92 000 (ethanol)	
	Rhodamine B	610	0.49 (ethanol)	106 000 (ethanol)	
	Texas red	615	0.93 (ethanol)	140 000 (ethanol)	
Fluorescent proteins	Cerulean	475	0.62	43 000	36
	T-sapphire	511	0.60	44 000	25
	mOrange	562	0.69	71 000	9.0
	mPlum	649	0.10	41 000	53
BPLPs	BPLP-Cys	437	0.62	133 (1,4-dioxane)	
	BPLP-Ser	441	0.32 (1,4-dioxane)	117 (1,4-dioxane)	
		535	0.12 (1,4-dioxane)	51 (1,4-dioxane)	
		540	0.02 (1,4-dioxane)	10 (1,4-dioxane)	

concentration or to be loaded in a condensed or solid phase. To alleviate ACQ effects, steric hindered groups, such as bulky cyclics, branched chains, and dendritic wedges have been conjugated onto fluorophores to impede aggregation formation.<sup>45</sup> With a specific molecule design, various aggregation enhanced emission (AEE) fluorescent materials have been obtained to address this issue.<sup>46,47</sup> The optical properties of some typical fluorescent materials were listed in (Tables 1 and 2 and Fig. 5). Autofluorescence from the examined objective is another concern. For *in vivo* imaging application, biological

tissue has strong light scattering and autofluorescence.<sup>48</sup> Plasma also has massive absorption at 400–670 nm (hemoglobin).<sup>49</sup> Therefore, a near infrared (NIR) fluorophore is usually preferred for tissue imaging to avoid an overlap with tissue-autofluorescence and light scattering/absorption.

From a physiological point of view, biocompatibility of the fluorescent materials has the first priority. Generally, traditional fluorescent probes, including organic dyes, quantum dots, and GFPs, have different degrees of cytotoxicity.<sup>50–53</sup> Conjugation with or encapsulation in polymers are the most common and

**Table 2** Comparison of properties among fluorescent materials

Property	Organic dyes	Quantum dots	Fluorescent proteins	BPLPs
Emission range	All range from UV to IR	All range from UV to IR (size dependent)	440–649 nm	434–725 nm
Molar extinction coefficient	$2.5 \times 10^4$ – $2.5 \times 10^5 M^{-1} cm^{-1}$	$10^5$ – $10^6 M^{-1} cm^{-1}$	$10^3$ – $1.5 \times 10^5 M^{-1} cm^{-1}$ (per chain)	$100$ – $200 M^{-1} cm^{-1}$
Quantum yield	0.5–1.0 (visible), 0.05–0.25 (NIR)	0.1–0.8 (visible), 0.2–0.7 (NIR)	0.10–0.79	0.02–0.62
Size/molecular weight	Up to 0.5 nm	6–60 nm	~27 kD	1000–1500 g mol <sup>-1</sup>
Fluorescent lifetime	1–10 ns	10–100 ns	1–10 ns	1–5 ns
Solubility	Depending on the chemical structure	Depending on surface chemistry	Can be water-soluble <i>via</i> a series of site-directed mutations	Different solubility based on various monomers
Bioconjugation	Using conjugation chemistry based on the functional group, usually multi-dyes on a single biomolecule	Well-established protocol of ligand chemistry	Can be conjugated easily <i>via</i> conjugation chemistry, due to the ubiquitous presence of cysteine and lysine residues	Rich of –COOH, and –OH group, which can be used for bioconjugation
Processability	Small molecule, usually loaded with a polymeric carrier	Normally used as a fluorescent label	Working individually as a biosensor, but not as any devices, like nanoparticles, scaffolds	Used for scaffolds, nanoparticles, and biosensors
Body clearance	Retention and clearance depending on dyes	<5.5 nm, rapid and efficient renal clearance; >15 nm, prevented renal excretion	Clearance from body <i>via</i> renal proximal tubules	Completely degradation into non-toxic monomers
Toxicity	Potential cellular toxicity due to the aromatic structure	Main issue for the use of QDots due to the heavy metal, and potential nanotoxicity	Generally nontoxic to cell, but still have issues due to the over-expression, and protein aggregation	Have the comparable toxicity with PLA

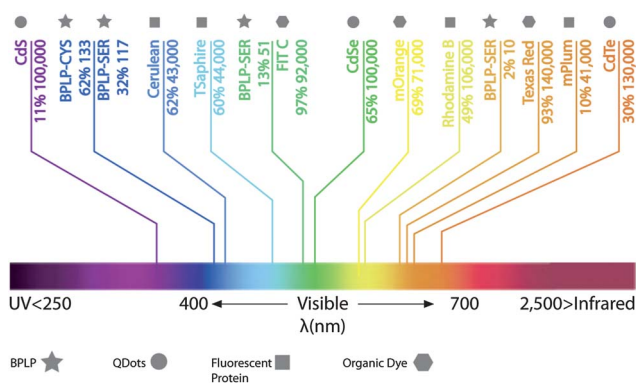


Fig. 5 Extinction coefficient, optimal emission wavelength, and corresponding quantum yield of different fluorescent materials.

effective way to considerably reduce the cytotoxicity. It has been found that polymer coating can effectively block the release of heavy metal ion from the core, which is considered the main course of its alarming cytotoxicity.<sup>54</sup> Polymers can also provide the potential for targeted delivery, and protection against a physiological environment. The dosage of fluorophore can be considerably reduced, in other words, lowering cytotoxicity. Although there is no standard protocol to evaluate biocompatibility of custom-made fluorescent materials, comparison with FDA approved ones in the same category is able to provide strong evidence. For example, biodegradable polymer should be compared with PLA, PGA, or PLGA. Indocyanine green (ICG) can be a standard to all organic dyes. To our knowledge, there is no FDA approved quantum dots as of now. However, the silicon based quantum dots, Cdots, have been recently approved by the FDA for a clinical trial.<sup>55</sup> Therefore, Cdots can be set as a control for all quantum dots. The body clearance should also be given great concern. Research has shown that a nanosphere with a dynamic diameter smaller than 5.5 nm can be rapidly cleared by renal. However, like a double-edge sword, rapid body clearance greatly reduces the toxicity, but it also increases the needed dosage of fluorophore for a sustained window. Biodegradable polymer seems like a perfect solution. An increased size after conjugation or encapsulation with polymers helps to avoid renal clearance. Some surface modification, such as PEGylation, confer propensity to evade scavenging by the Reticuloendothelial system (RES).<sup>56</sup> Thus, a prolonged window period can be obtained while everything can still be renal clearable after the full degradation of polymers.

Meanwhile, the physicochemical property can also be improved by incorporation of biodegradable polymers. Due to the aromatic nature of organic dyes and hydrophobic surface of Qdots from synthesis, conjugation with water-soluble polymer or encapsulated with polymeric colloids will considerably increase their aqueous solubility. Aggregation stability of the fluorophore should also be concerned. For examples, Qdots with smaller size and damaged surface shield exhibit low stability against aggregation.<sup>54,57</sup> Moreover, a negative surface charge also causes unexpected ionic interactions with a biological environment.<sup>54</sup> Sufficient free functional groups are also crucial due to the need for further conjugation of multiple

moieties, such as PEG, drug, and targeting moiety. Although numerous derivatives of traditional organic dyes have been synthesized with functional groups present, the limited number of functional groups hinders multiple conjugations for various purposes such as targeting and longer circulation time. Incorporation of a fluorophore into biodegradable polymers with sufficient functional groups, such as PLGA, poly(L-glutamic acid), and PCL, has been a common solution for the above concern.

## 4 Organic dye-enabled biodegradable fluorescent polymers

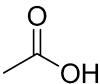
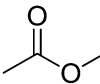
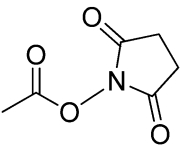
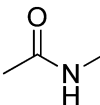
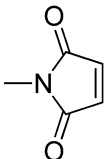
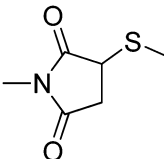
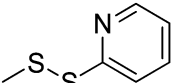
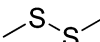
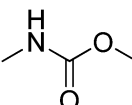
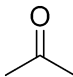
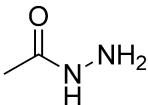
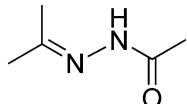
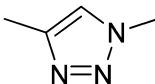
The first synthetic organic dye, Mauveine, was discovered by William Henry Perkin in 1856. It has been proven to be effective in dyeing silk and textiles. Since its inception, thousands of organic dyes have been prepared for a wide range of applications. For bioimaging purposes, a large number of organic dyes have been developed to examine the fundamental processes at the organ, tissue, cellular, and molecular levels.<sup>12,58</sup> Based on chemical structure, they can be divided into several classes, cyanine, porphyrin, squaraine, BODIPY, and xanthenes. All the commonly used dyes are derivatives from these classes, such as indocyanine green from cyanine, fluorescein and rhodamine B from xanthenes. In order to meet the requirement for different biomedical applications, various chemical modifications have been made upon traditional dyes to tune emission wavelength, increase fluorescence intensity, and introduce functional groups. A series of commercial organic dyes have been developed, such as Cy® and Alex Fluor® by Molecular Probes, and DyLight® by Thermo Fisher Scientific.

Of all the currently available organic dyes, only indocyanine green (ICG) has been approved by the FDA for clinical use as diagnostic agents. Bare organic dyes tend to be non-specific to target tissue, unstable, toxic, and rapidly cleared from the body. Major limitations of bare organic dyes include the potential carcinogenesis, which comes from aromatic structure, low threshold of photobleaching, and the lack of functional groups for further conjugation. Incorporation with biodegradable polymers shows great potential to solve these obstacles. In the present section, two approaches will be discussed thoroughly. One is single water-soluble macromolecule conjugation, and the other is encapsulation with polymeric colloids. Organic dye-conjugated polymeric scaffold will also be discussed.

### 4.1 Conjugation chemistry

Before reviewing the conjugates of polymer and organic dye, an overview of conjugation chemistry should first be summarized. Various conjugation strategies have been developed covering all the functional groups that exist in organic dyes and biodegradable polymer. The most commonly used conjugation chemistry is listed in Table 3. The carboxyl group is present in many biodegradable polymers, most of which are synthesized *via* ring-opening polymerization, such as PGA, poly( $\alpha$ -malic acid), and their copolymers. The carboxyl group can be easily activated by carbodiimide for conjugation.

**Table 3** Commonly used conjugation chemistry in biomedical application

Functional group	Conjugating group	Crosslinking chemistry	Final group
	—OH	Carbodiimide (EDC, DDC)	
—NH <sub>2</sub>		NHS ester	
—SH		Maleimide	
		Pyridyl disulfide	
—OH	—N=C=O	Isocyanate	
		Hydrazide	
—C≡CH	—N <sub>3</sub>	Click chemistry	

*N,N'*-Dicyclohexylcarbodiimide (DCC) is suitable for a water insoluble condition, while 1-ethyl-3-(3-dimethylaminopropyl) carbodiimide (EDC) is for an aqueous environment. Although carbodiimide is able to conjugate both the carboxyl and amino groups, *N*-hydroxysuccinimide ester (NHS-ester) is more specific to amidation. The thiol group has its specialty in quantum dot chemistry, and is present in many proteins and peptides. Meanwhile, thiolation for different molecules has been well established in organic chemistry. Polymers with maleimide and pyridyl disulfide can be conjugated with thiolated molecules. Hydroxyl groups can also be found in many organic compounds. Except for carbodiimide chemistry, the hydroxyl group can react with the isocyanate group to form a urethane bond in an active -H free environment. In addition, the hydroxyl group can also be oxidized into the aldehyde group by some mild oxidant, such as sodium periodate. Then aldehyde groups can be conjugated with the hydrazide group. Recently, click chemistry has been extensively studied due to the easy introduction of azides and alkynes.<sup>59</sup> Reaction can be conducted in a wide range of solvents (including water). Although the use of a Cooper-based catalyst has been a concern for biomedical application, catalyst free click chemistry has been well established recently.<sup>60</sup>

#### 4.2 Water-soluble fluorescent polymers

Tremendous efforts have been made to prepare polymer-dye conjugates. The conjugates have several advantages over the bare organic dyes: (1) since the major content of organic dyes is their aromatic structure, which is usually non-water soluble, conjugation with a water soluble polymer can dramatically increase the hydrophilicity; (2) conjugation with a polymer can protect dyes from rapid metabolism and body clearance; and (3) polymer provides additional functional groups for conjugation of targeting and therapeutic moieties. With the rapid growth of pharmaceutical and material science, various polymers have been considered for the formulation. To include the above benefits in one formulation, the chosen polymer should meet several requirements: (1) biocompatible; (2) water solubility; (3) biodegradable for body clearance; and (4) having functional groups that can be reacted with organic dye and conjugation with other molecules, such as drugs and targeting moieties.

Among numerous water soluble polymers, poly(ethylene glycol) (PEG) is the most commonly studied polymer, and its pro-drug formulation with an anti-cancer drug has received regulatory approval in different countries.<sup>61</sup> The end-group



chemistry of PEG has been intensively studied. PEG with different molecular weight and with different end groups are commercially available, or can be synthesized with reported protocol. Multi-armed PEG provides the multiple conjugation sites for different functional molecules. Although PEG is not biodegradable, it can be served as a standard for PEG-based polymers and many other water soluble polymers. Meanwhile, many efforts have been put on the strategies to produce biodegradable derivatives of PEG. Zhao *et al.*<sup>62</sup> described the synthesis of biodegradable multiarm PEGs, and it has entered clinical trials. Poly(L-glutamic acid) (PG) is a biodegradable polymer and its breakdown product, L-glutamic acid, can enter normal cellular metabolism. Every repeating unit has carboxyl groups, so PG has sufficient sites for conjugation. The pro-drug of PG and Paclitaxel is now under phase III clinical development in the U.S.<sup>6</sup> Melancon *et al.*<sup>63</sup> conjugated PG with a cyanine derivate, near infrared dyes (NIRF). After conjugation of NIRF, there are still numerous free carboxyl groups for conjugation of targeting moieties and drugs. Although this PG-NIRF was used to study *in vivo* degradation of PG based polymer-drug conjugates, it showed great potential for whole body imaging or tumor imaging. A number of biodegradable *N*-(2-hydroxypropyl)methacrylamide (HPMA) based copolymers (co-pHPMA) caught much attention over the last 30 years.<sup>64</sup> Co-pHPMA can be conjugated with different imaging moieties through copolymerization and chemical conjugation. Jensen *et al.*<sup>65</sup> conjugated co-pHPMA with fluorescein-cadaverine, and used it to study the intracellular metabolism of the copolymer. Dextran is another polymer that has been conjugated with organic dyes for imaging. Helmchen and Denk<sup>66</sup> used dextran-FITC/rhodamine conjugates for high resolution brain imaging. The vicinal diol structure could be oxidized by periodate and further conjugated with various functional molecules.<sup>67</sup>

In addition to linear polymers, dendrimer is a class of branched macromolecules forming a star-like structure. The physiochemical properties can be easily tuned due to its step-wise fashion synthesis. Theoretically, generation 5 (G5) dendrimers will have 128 free functional end-groups on the surface. Thus, a high density of functional groups on the outer layer of dendrimer confers sufficient sites for the conjugation of organic dyes, targeting moieties, and drugs. A major advantage of dendrimers over a linear polymer is that hydrophobic molecules can be encapsulated in the cavity formed by an adjacent branch.<sup>68</sup> Some dendrimers with positive surface charges, such as poly(ethyleneimine), have also been investigated as carriers for negatively charged DNA.<sup>69</sup> Polyamidoamine (PAMAM) is the most commonly used dendrimer. Biodegradable PAMAMs were prepared by many labs *via* different strategies, and have been used for drug delivery and gene therapy.<sup>70</sup> Majoros *et al.*<sup>71</sup> conjugated fluorescein isothiocyanate (FITC) onto PAMAM, and investigated it for both *in vivo* and *in vitro* imaging. Interestingly, some of PAMAMs have been found to have fluorescent properties.<sup>33,34,72</sup> The fluorescent mechanism has been discussed above. This unique property makes PAMAM a dye-free imaging probe. Therefore, complexity of the design can be greatly reduced.

### 4.3 Methods of dye incorporation into biodegradable polymers

With the rapid development of biodegradable polymeric colloids, immense studies have been focused on incorporating organic dyes with those colloids for various bioimaging applications, especially polymeric nanoparticles for cancer imaging. Generally, organic dyes can be combined with polymer colloids *via* two different ways, chemical conjugation and physical encapsulation.

**4.3.1 DYE ENCAPSULATION.** Biodegradable polymers can be fabricated into nanoparticles of different structures, such as nanocapsules, nanospheres, and micelles depending on physicochemical properties of polymers and fabrication techniques. Nanocapsule is a core-shell structure with a polymer membrane and cavity inside, which can be a reservoir for organic dyes, whereas nanosphere is a polymeric matrix in which the dye molecule can be evenly dispersed. Polymeric micelles can be self-assembled in an aqueous solution by amphiphilic polymers. Diblock, triblock, and random copolymers of both hydrophobic and hydrophilic blocks can self-assemble into micelles. They have a generally small size (<100 nm), depending on the critical micelle concentration (CMC), and a propensity to evade scavenging by the reticuloendothelial system (RES). Those structures confer protection to an organic dye and considerably improve the stability. Targeted delivery can also be achieved by surface conjugation of targeting moieties. Organic dye encapsulated nanoparticles have been generally exploited for the study of pure imaging purposes, such as cellular uptake, intracellular fate, metabolism, and biodistribution.<sup>73-75</sup>

**4.3.2 CHEMICAL CONJUGATION.** Biodegradable polymeric colloids have been intensively investigated as a delivery vehicle for drugs, genes, proteins, and cells. To save more loading space for those components and avoid interference with the aromatic fluorophore, organic dyes are chemically conjugated with polymeric colloids either during the synthesis of polymers or *via* surface conjugation of polymeric colloids. Poly(alkyl cyanoacrylate) (PACA) and its copolymers are a family of biodegradable polymers. Droumaguet *et al.*<sup>76</sup> synthesized PACA copolymers by three monomers, hexadecyl cyanoacetate, methoxypoly(ethylene glycol) cyanoacetate, and rhodamine B conjugated cyanoacetate. The fluorescent intensity can be tuned by varying the feeding ratios of dye conjugated monomers. The resulted amphiphilic polymers were self-assembled into nanoparticles. Those nanoparticles have been demonstrated suitable for *in vitro* imaging of human brain endothelial cells. Numerous biodegradable polymeric colloids have functional groups on the surface, such as colloids made from PLGA, Poly(L-glutamic acid), poly( $\epsilon$ -caprolactone) (PCL), and their amphiphilic copolymers with PEG as a hydrophilic block, as well as nature polymers, such as chitosan, and gelatin. PLGA nanoparticles have been surface labeled with FITC, Cy®, Alex Fluor®, and Rhodamine for various imaging studies.<sup>77-79</sup> The label of Near-Infrared cyanine dye (NIR-797) helped the real-time biodistribution study of PCL based micelles.<sup>80</sup> For natural polymer-based nanoparticles, Nam *et al.*<sup>81</sup> conjugated Cy5.5 was labeled on the surface of chitosan nanoparticles. This fluorescent nanoparticle

has been successfully used for the study of nanoparticle biodistribution and tumor accumulation.

#### 4.4 *In situ* imaging of biodegradable fluorescent polymeric scaffold

With the rapid development of biodegradable polymers for *in situ* tissue engineering, non-invasively or minimal-invasively monitoring the behavior of polymeric implants becomes crucial. Although the properties of biodegradable polymers have been carefully evaluated *in vitro*, such as degradation speed and mechanical properties, understanding these material properties *in vivo* remains elusive as the physiological environment provides a more complicated degradation or erosion than *in vitro*. There is an urgent need to assess material properties *in situ* and in real time.

Recently, Edelman *et al.*<sup>82</sup> presented a decent study on tracking polymeric scaffold using fluorescence imaging. In this study, fluorescein was conjugated onto PEG, and then mixed with dextran to form fluorescent hydrolyzable hydrogel. Enzymatically degradable collagen labeled with Texas-red was also used to assess its enzymatic degradation. *In vitro* and *in vivo* degradation were both performed for comparison. It was found that the *in vivo* hydrolytical degradation rates of the PEG-based scaffolds could well correlate with the *in vitro* degradation of the samples, while the enzymatic degradation of collagen samples has a more complicated behavior in different sites of the body. This study represents an advance in tissue engineering where there has been a dearth of understanding on the scaffold degradation and tissue replacement *in situ* and in real time. Fluorescent scaffolds enable a real-time quantitative evaluation of the scaffold evolution over time *via* a fluorescence imaging method. This study also implies the added fluorescent properties can be beneficial in the design of the next wave of tissue engineering scaffolds to function as both implants and imaging probes.

## 5 Inorganic dyes enabled biodegradable fluorescent polymers

Generally, naked Qdots are not ready for bioimaging due to the easy surface oxidation, insufficient functional groups, and most importantly the water-insolubility.<sup>54</sup> To address these problems, polymers have been introduced to make Qdots more suitable for bioimaging. Various polymers can be incorporated with Qdots focusing on the different facets of benefits, such as greatly increasing the stability and hydrophilicity of Qdots, lowering the toxicity, offering sufficient sites for further modification, and providing a reservoir for drug loading.<sup>83</sup> As illustrated in Fig. 6a, polymer coating converts the hydrophobic surface of Qdots to hydrophilic. Fig. 6b showed that the tunable fluorescence of Qdots has been investigated for multicolor fluorescence imaging of cancer cells under an *in vivo* environment. The polymer layer also improves the colloidal stability and lowers the chance of aggregation.<sup>84</sup> In addition, a simple polymer coating has proved to act as a significant barrier for heavy metal ion ( $\text{Cd}^{2+}$ ) diffusion, which was considered a major

cause of toxicity of Qdots.<sup>54</sup> Polymers with various functional groups, such as amine, carboxyl group, and maleimide, can be exploited to further conjugate with antibodies, peptides, hydrophilic therapeutics, or aptamers. From a therapeutic point of view, the polymer network provides sufficient room for the hydrophobic drug compared to the solid semiconductor component of Qdots, which is simply an imaging probe. A large pool of polymers has been studied to encapsulate or conjugate with Qdots *via* various techniques.<sup>30</sup> All those techniques can be classified into two ways, surface coating and bulky embedding. There are also numerous studies on incorporating Qdots with inorganic substances, such as silica or titania, non-biodegradable polymers, such as poly(maleic anhydride *alt*-1-tetradecene), and dendrimers, such as poly(amido amine).<sup>85,86</sup> However, we will only focus on the strategies of incorporating inorganic dyes with biodegradable polymers below.

### 5.1 Biodegradable polymer coating on Qdots

Qdots are usually characterized for their photophysical properties, such as emission wavelength, quantum yield, photostability, and physicochemical properties, such as size, surface charge, and aggregation stability. Both of them may change after surface coating with biodegradable polymers.<sup>54</sup> There are two distinct strategies usually adopted for Qdot coating: ligand exchange and ligand capping.

**5.1.1 LIGAND EXCHANGE.** The ligand exchange strategy involves completely replacing the surface bound ligands remaining during the decomposition of metal-organic or organometallic precursors at elevated temperatures.<sup>87</sup> Those ligands include trioctylphosphine oxide (TOPO) and lipophilic trioctylphosphine for most cases. Physicochemically, the advantage of ligand exchange is maintaining the small final diameter. Choi *et al.*<sup>88</sup> pointed out that Qdots with a hydrodynamic diameter smaller than 5.5 nm can be cleared rapidly from the body by renal filtration and urinary excretion. Therefore, keeping a small final diameter after surface coating can be beneficial in reducing toxicity. However, Qdots with a small diameter after ligand exchange suffer from low stability against aggregation.<sup>54</sup> From a photophysical point of view, replacing the original ligand of Qdots may result in several disadvantages. The exchange process raises the risk of surface damage of Qdots, leading to a decrease of quantum yield. It also increases the likelihood for surface oxidation, which will lead to poor photostability and a blue shift of emission wavelength.

Since there is a specific interaction between the thiol group and heavy metal, such as gold, silver, cadmium and so forth, thiolated polymers are the most common ligands involved in the ligand exchange strategy.<sup>89</sup> Thiolated PEG has been extensively exploited due to its ease of synthesis, ease of handling, and versatile applications. Hou *et al.*<sup>90</sup> reported a disulfide bond-bearing and symmetric PLLA-SS-PLLA synthesized by ring-opening polymerization, and its reduced product PLLA-SH. The thiolated PLLA has been successfully coated onto CdSe with the ligand exchange strategy. A quantum yield of 53% was reported by tuning the molecular weight of PLLA-SH, and the feeding ratios between ligand and Qdots. The hydroxyl groups

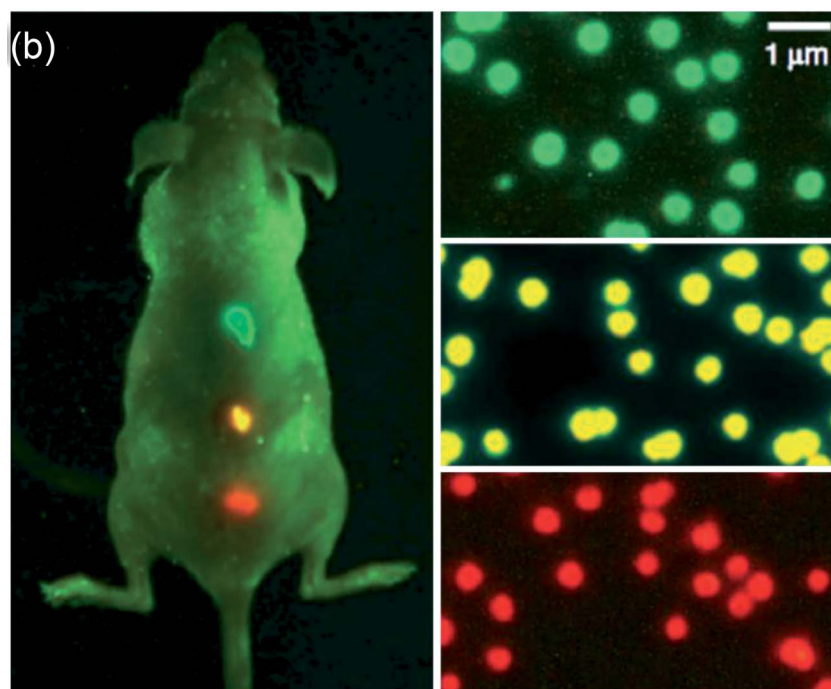
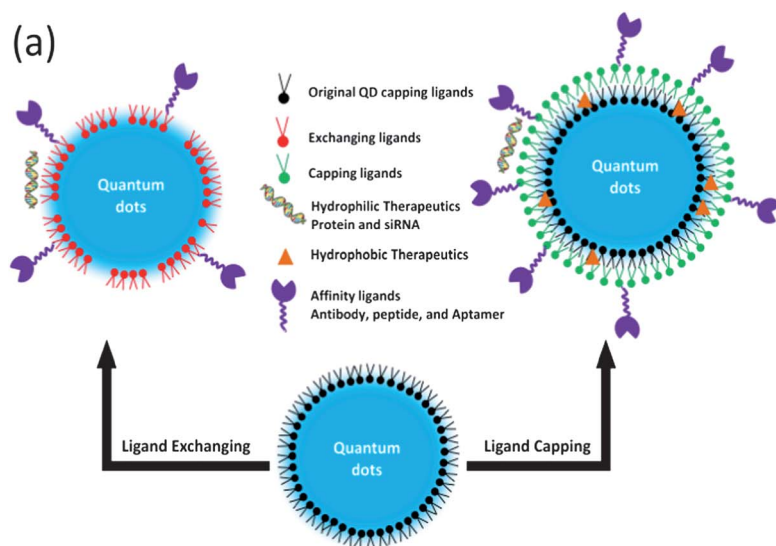


**Fig. 6** (a) Schematic illustration of multifunctional Qdots coated with biodegradable polymers. (b) Cellular and animal imaging showing Qdots with different colors under the same light source.<sup>27</sup>

on the other end of PLLA-SH also provide sites for further conjugation. The synthesis of thiolated PLLA sets as a protocol for thiolation of various biodegradable polymers that can be synthesized through ring-opening polymerization, such as family of cyclic lactone, and morpholine-2,5-dione.<sup>3</sup> Except for the thiol group, amine bond and phosphine bond have also been exploited for ligand exchange.<sup>54</sup> However, rarely has any biodegradable polymer been reported involving the latter two chemical groups.

**5.1.2 LIGAND CAPPING.** Different from ligand exchange, ligand capping only caps the original ligands on Qdots with suitable amphiphilic polymers. Without damaging the

protecting ligands of Qdots, the photophysical property will be better retained. The thicker layer of coating provides not only a better protection against surface oxidation but also a good chemical stability and a reliable protection against aggregation. Typically, the coating will also increase the particle size by as much as 5–10 nm.<sup>91</sup> This number depends on the molecular weight of both hydrophilic and hydrophobic blocks. A larger size of Qdots after ligand capping may have a low renal clearance. However, the bare Qdots still can undergo renal clearance after polymer coating is fully degraded. On the other hand, a longer circulation time can extend the targeting and potential drug delivery window once injected in the blood circulation.

The surfaces of naked Qdots are occupied by hydrophobic ligands from the organometallic compounds during the syntheses of Qdots, such as the stabilizing ligand, trioctylphosphine oxide (TOPO), or hexadecylamine.<sup>92</sup> A ligand capping strategy exploits the physical interaction between a hydrophobic ligand from Qdots and a hydrophobic part of an amphiphilic polymer. After the first successful case of coating amphiphilic polymers on Qdots by Dubertret *et al.*,<sup>93</sup> many others have explored this approach to coat Qdots with small organic molecules and non-degradable polymers. Although there have been extensive research on biodegradable amphiphilic block copolymers,<sup>94</sup> very few studies have been reported on coating Qdots with these polymers *via* physical interactions due to their weak binding. Stabilization of the coating layer has been proved by crosslinking the coating polymers. Various crosslinking methods have been introduced to stabilize the polymer layer, such as lysine or diamine for polymers with an abundant carboxylic group, and free radical crosslinking for polymers with an abundant double bond.<sup>54</sup>

Currently, most studies have focused on non-degradable amphiphilic polymers. Nevertheless, those studies provided general protocols for coating biodegradable polymers on Qdots *via* ligand capping. Pellegrino *et al.*<sup>95</sup> have reported a general route to coat various Qdots with poly(maleic anhydride *alt*-1-tetradecene) *via* ligand capping, and further crosslinked the layer with bis(6-aminoethyl) amine. Gao *et al.*<sup>27</sup> reported that CdSe/ZnS was coated with a triblock copolymer consisting of a polybutylacrylate segment, a polyethylacrylate segment, and a polymethacrylic acid segment. The polymer layer was further crosslinked by peptide. These polymer coated Qdots showed great potential in cancer imaging. These reports can serve as standard approaches for any -COOH containing biodegradable amphiphilic polymers, such as PEG/PLGA and PEG/poly(aspartic acid).

## 5.2 Qdots-embedded biodegradable polymers

A number of studies have attempted to embed Qdots into polymers such as polymeric nano/microparticles and micelles. Similar to organic dye incorporation, techniques of incorporating Qdots in polymers can be divided into two methods: chemical bonding and physical encapsulation.

To chemically bond Qdots with biodegradable polymers, functional groups should be introduced on Qdots first, which can be achieved with either ligand exchange or ligand capping strategies. Different from organic dyes, Qdots can be chemically bonded to polymer colloids during polymerization. Various polymers can be synthesized and form particles *via* emulsion and dispersion polymerization. Many studies successfully demonstrated the incorporation of Qdots into polymer colloids.<sup>96</sup> During the process, Qdots are required to be dissolved in oil droplets. In other words, there is no need for surface modification of Qdots to make them hydrophilic. However, polymers that are applicable for emulsion polymerization are normally non-degradable. Interestingly, a biodegradable polyurethane nanoparticle was fabricated *via* miniemulsion techniques by Cramail *et al.*<sup>97</sup> Although no

further research has been conducted on these polyurethane nanoparticles, it represents a new way of synthesizing biodegradable polymer colloids in the presence of Qdots.

Although conjugating Qdots onto the surface of polymer spheres has been rarely reported, Yeh *et al.*<sup>98</sup> reported Qdots conjugated PLGA nanoparticles as a potential candidate for gene delivery. By conjugating the nuclear localization signal (NLS) on the surface of nanoparticles, HeLa cells exhibit fluorescence at the nuclei region after incubating with the NLS-nanoparticles. However, Qdots are normally encapsulated inside the polymer sphere due to their relatively poor stability and potential cellular toxicity. Like organic dyes, Qdots can be encapsulated into biodegradable polymeric colloids *via* different fabrication techniques. Desai *et al.*<sup>99</sup> encapsulated CdSe/Zns into PLGA nanoparticles *via* nanoprecipitation. Kim *et al.*<sup>100</sup> encapsulated CdTe/CdSe into PLGA nanoparticles *via* a double emulsion technique. The Qdots loaded nanoparticles have a similar value of quantum yields to the bare Qdots (52%), and the emission wavelength remained the same (760 nm). Another group also reported the encapsulation of protein-conjugated Qdots into PLGA *via* a double emulsion technique.<sup>101</sup> The carboxylic groups on the polymers were conjugated with Herceptin, a monoclonal antibody that targets ErbB2 cell membrane receptors. Specific targeting to ErbB2-positive SKBR3 breast tumor cells and intracellular controlled release of quantum dots was achieved. As we discussed above, amphiphilic copolymers have been intensively studied for the surface modification of Qdots. Due to the ability to self-assemble into micelles, those copolymers have been used for encapsulation of Qdots. Due to the hydrophobic core/hydrophilic shell structure of micelles, Qdots can be distributed within the hydrophobic core. Cao *et al.*<sup>102</sup> reported a PbS loaded *N*-succinyl-*N'*-octyl chitosan micelles for targeted imaging of liver cancer. The emission wavelength of PbS loaded micelles presents a red shift (800–870 nm) due to the stabilization and energy transfer of Qdots. The unnoticeable toxicity both *in vitro* and *in vivo* implied that low leakage of QDs from the micelle. However, the long term toxicity of the micelle needs to be further studied. After 12 h of intravenous injection, micelle has been found to accumulate at a tumor site *via* an enhanced permeability and retention (EPR) effect. The strong fluorescence can be observed up to 96 h. Liu *et al.* loaded hydrophilic CdSe/ZnS into PLA-*b*-poly(2-methacryloyloxyethylphosphorylcholine) (PLA-*b*-PMPC). TEM imaging indicated that most of the Qdots were located in the core of nanoparticles.

Stimulus-responsive polymers have also been used to load Qdots. The external stimulus can trigger the conformation change of those polymers. The most notable stimulus-responsive polymers are pH or temperature sensitive ones. The mechanism of loading Qdots in such polymers is an expansion-uptake/shrink-entrap process. Xu *et al.*<sup>103</sup> reported a pH-sensitive copolymer of *N*-isopropylacrylamide and 4-vinylpyridine (PNIPVP), and the loading of CdTe into the PNIPVP nanoparticles. Qdots were loaded during expansion of the PNIPVP nanoparticle under pH 3, and entrapped within the particles at pH 3–10. Eventually, the Qdots can be released when pH > 11. Poly(*N*-isopropylacrylamide) (PNIPAM) also proved to be

thermo-sensitive. When the temperature is below a lower critical solution temperature (LCST), PNIPAM microparticles expand. Therefore, they are able to entrap Qdots, when temperature is higher than LCST. However, the release of Qdots remains a problem when the temperature is lowered below LCST. Gong *et al.*<sup>104</sup> loaded CdTe into PNIPAM microparticles, and exploited the hydrogen bonding between surface ligands from CdTe and amide groups from PNIPAM to stabilize the loaded Qdots. Although PNIPAM and its copolymers are not biodegradable, these studies serve as good references for Qdots embedded in various biodegradable pH or thermo-sensitive polymers. A number of polypeptides with pendant ionizable groups present a pH-sensitive property, such as poly(aspartic acid), poly(glutamic acid), polyarginine, polyhistidine, polylysine, and their copolymers.<sup>3</sup> Meanwhile, many PNIPAM based polymers have been proved to be biodegradable. Biodegradable PNIPAM-*b*-PLA has been synthesized by ring-opening polymerization of lactide initiated by PNIPAM-OH.<sup>105</sup> A similar approach has been used to prepare PNIPAM-*b*-poly(glutamic acid) and PNIPAM-*b*-poly(L-lysine).<sup>3</sup> Radical polymerization techniques, including Reversible Addition-Fragmentation chain Transfer (RAFT), and Atom transfer radical polymerization (ATRP), have been used to prepare PNIPAM-based copolymers, such as a PNIPAM-poly(3-hydroxybutyrate)-PNIPAM triblock copolymer.<sup>3</sup> All these polymers could potentially be used for Qdots embedding.

## 6 Green fluorescent protein

In 1956, Shimomura *et al.* discovered green fluorescence from *Aequorea* jellyfish as a companion protein to aequorin. Since

then, this green fluorescent protein (GFP) has become one of the most useful biological tools in the past decade.<sup>35,106</sup> The primary structure of *Aequorea* GFP was deduced from the cDNA sequence. *Aequorea* GFP is a protein of 238 amino acids with a molecular weight of 27 or 30 kDa. The chromophore of GFP is formed from the primary amino acid sequence, residues 65–67, which are Ser-Tyr-Gly (Fig. 3a). After conformational folding and a series of reactions, including cyclization, dehydration, and oxidation, the chromophore, (*p*-hydroxybenzylidene)-5-imidazolinone is formed. This structure has later been confirmed by two-dimensional NMR and the cDNA sequence.<sup>35</sup> To fulfill the requirements for various applications, tremendous efforts have been placed on preparing yellow and red fluorescent proteins. The GFP variants can be classified by different emission colors, from cyan (475 nm) up to far-red (649 nm).<sup>39</sup> Shaner *et al.*<sup>38,39</sup> have made significant contributions to the family of GFP, such as the only bright and photostable far-red FP, mPlum, superior photostable red FP, mCherry, brightest orange FP, mOrange, yellow FP, mCitrine, brightest cyan FP, Cerulean, and the UV-excitable GFP, T-sapphire (Fig. 3b).

The most important advantage of GFP is that it can be genetically encoded into protein and expressed in living cells and organisms.<sup>107</sup> Due to this distinct benefit, GFP has been extensively used as an intrinsic intracellular indicator of a specific protein, other than an imaging probe for many drug/gene delivery systems. There are rarely any reports on combining GFP with biodegradable polymers. The criteria on how to choose a fluorescent protein and specific application of GFP has been summarized elsewhere.<sup>38</sup> GFP has been exploited

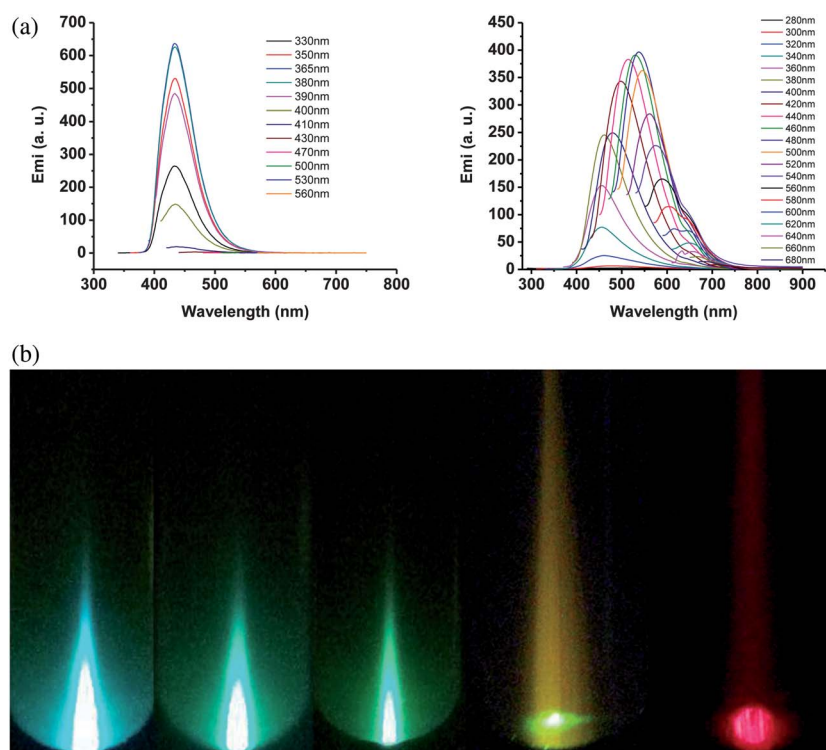


**Fig. 7** Emission spectra of BPLP-Cys (a) and BPLP-Ser (b) at different excitation wavelengths. (c) BPLP-Ser solution emits different colors, blue, cyan, green, yellow and red (from left to right) with laser excitation.

as pH sensitive and redox sensitive indicator for dynamic intracellular activity. Based on the variety of fluorescent proteins, there are many chances of crosstalk in excitation and emission channels from two fluorescent proteins, which confers a great opportunity for fluorescence resonance energy transfer (FRET) on a pair of fluorescent proteins.<sup>108</sup> The FRET effect of fluorescent proteins has been exploited for studying protease action and  $\text{Ca}^{2+}$  sensitivity.<sup>109</sup>

## 7 Biodegradable photoluminescent polymers

All previous studies have to utilize either organic dyes or other fluorescent agents to confer fluorescent properties to biodegradable polymers. Recently, the authors' laboratory has made a breakthrough on synthesizing a new family of biodegradable photoluminescent polymers based *via* a convenient polycondensation reaction.<sup>40</sup> Briefly, a diol such as 1,8-octanediol, citric acid, and  $\alpha$ -amino acid were reacted to form a pre-polymer (pre-BPLP). All 20 essential  $\alpha$ -amino acids and their derivatives have been used for the syntheses of BPLPs all of which showed remarkable fluorescence. All three monomers used for synthesis are non-toxic. The multifunctional monomer citric acid is a non-toxic metabolic product of the human body (Krebs or citric acid cycle).<sup>110</sup> There is no reported toxicity for 1,8-octanediol. Amino acids are critical to life, and play an important role in metabolism. As the most basic units for protein, amino acids are water-soluble and biocompatible.

With a polyester backbone, pre-BPLP can be degraded in PBS within 16 d. The fluorescence intensity decayed with the degradation, and completely died out after the polymers were fully degraded. The complete degradation also eliminates the concern of the toxicity raised by accumulation in tissue. Compared with a traditional organic dye, rhodamine-B, BPLP-Cys only lost less than 2% of its original fluorescent intensity after 3 h continuous UV excitation, which is significantly lower compared to a 10% loss of rhodamine-B. Based on our systematic studies on BPLPs with different amino acids, BPLPs have a high quantum yield, up to 62.3%, which is BPLP-Cys. The higher quantum yield of BPLP-Cys over other amino acids is because of the formation of a double bond which extends the conjugation system. The release of hydrogen sulfide was confirmed by  $\text{H}_2\text{S}$  test strips (Fig. 4c). This high quantum yield

is comparable to the CdTe/ZnS quantum dots, which is regarded as a bright fluorescent agent,<sup>11,58</sup> and is much higher than that of GFP.<sup>35</sup> The study of BPLP-Ser showed that it has a tunable emission by changing excitation wavelength, up to 700 nm, which is different from BPLP-Cys (Fig. 7a and b). The BPLP-Ser solution can emit different colors, from blue to red, under laser excitation (Fig. 7c). This unique property promises a great potential of BPLP-Ser as not only a NIR imaging material but also a candidate for multiplex imaging. The cytotoxicity study of BPLP showed that it has a comparable cyto-compatibility to PLGA 75/25. The *in vivo* evaluation also proved that there is no noticeable edema and tissue necrosis. A thin fibrous capsule and a weak chronic inflammatory response have been observed after 5 months of implantation for the crosslinked BPLP.

Different from the dye/polymer system reviewed above, BPLP has both a high molecular weight and fluorescence as one material. Therefore, BPLP is free of aromatic structure and heavy metal, in other words, reduced cytotoxicity. Due to its good processability, BPLP can be fabricated into micro/nanoparticles, films, and porous scaffold. Fluorescence is sustained after fabrication. Inherited from polymer, BPLP nanoparticles exhibit a strong, tunable, stable fluorescence for *in vivo* imaging (Fig. 8a). BPLP nanoparticles fabricated by nanoprecipitation have sizes around 100 nm. The degradation speed of BPLPs can be adjusted to control the drug-releasing rate. The abundant functional group, such as amine, carboxylic, and hydroxyl groups, provide sufficient sites for further conjugation. On the other hand, BPLPs can be fabricated into film, porous scaffold, and other devices by thermal crosslinking to meet the versatile needs of biomedical application. Fig. 8b showed that fluorescence of a BPLP-Ser porous scaffold can be clearly observed *in vivo*. Comparing to the dye conjugated polymers for real-time tracking of *in vivo* degradation,<sup>82</sup> the fluorophore of BPLP is more evenly distributed, and degradation can potentially be more accurately correlated with the decrease of fluorescence. In other words, unlike other fluorescent agents such as organic dyes and Qdots which simply only act as imaging agents, BPLPs also function as implants or devices, thus more potent in many biomedical applications.

Understanding the fluorescence mechanism will enable us to expand the biodegradable photoluminescent polymer into different classes of functional polymers. It is well known that  $-\text{OH}$  may initiate ring-opening polymerization to synthesize biodegradable polymers, such as PLA, PGA, and their copolymers. By controlling the molar ratio of citric acid/diol, we will be able to make a BPLP oligomer with the  $-\text{OH}$  group capped on both ends of the polymer chains, and exploit it as a starter for ring-opening polymerization. Moreover, without interrupting fluorophores, various monomers with functionality can be introduced to BPLPs. Hydrophilicity can be increased by partially or fully replacing diol with PEG. Hydrophilic BPLPs can be further reacted with regular hydrophobic BPLPs to form amphiphilic copolymer for self-assembling micelles. A double bond can be incorporated by maleic acid to make BPLPs photocrosslinkable (injectable). Urethane bond can be introduced to extend BPLPs to dramatically increase the mechanical

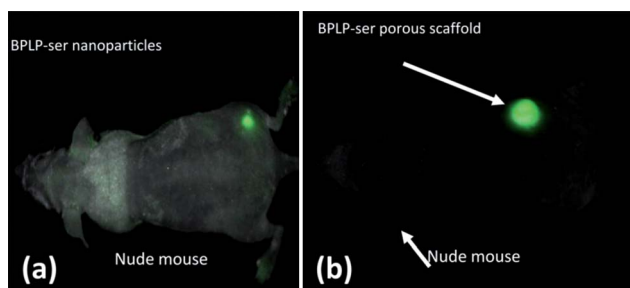


**Fig. 8** (a) Fluorescence image of BPLP-Ser nanoparticles injected subcutaneously in a nude mouse. (b) Fluorescence image of BPLP-Ser porous scaffold implanted subcutaneously in a nude mouse.

property. A novel methodology for synthesizing different classes of citric acid-based biodegradable photoluminescent polymers can be developed based on our understanding of the fluorescence mechanism.

## 8 Conclusion and perspectives

In the present reviews, we have summarized the design and applications of both fluorescent dye enabled biodegradable materials and biodegradable materials with intrinsic fluorescence. Biodegradable polymers were endowed with important missions to improve fluorescent dyes, such as protecting, stabilizing, reserving, functionalizing, and enabling the therapeutic ability. The biodegradability leads to complete body absorbance or clearance of those polymers after their missions were accomplished. Biodegradable polymers with intrinsic fluorescence (BPLPs) make one stride of improvement. It cuts off the design complexity and reduces the potential cytotoxicity from both organic and inorganic dyes. It is a ready to use material with low cost-efficiency and processing verities (injectable hydrogel, scaffold, film, and micro/nanoparticles). Those promising properties make BPLPs become the next generation fluorescent materials.

With the advances in synthetic organic chemistry, biodegradable polymers can be manipulated to have more and more promising properties. Recently, a smart design has been massively introduced to building polymers and enabling fluorescent switch. According to the difference between normal tissue and targeted tissue, redox, pH, and thermo sensitivities have been incorporated into biodegradable polymers to make them stimulus responsive. Therefore, on site activities of targeted tissue can be achieved, such as drug release and generating a fluorescent signal. Fluorescence resonance energy transfer (FRET) has begun to attract attention for its unique behavior that can switch on/off fluorescence. FRET of a pair of fluorescent proteins has been widely used for tracking physiological activities. In the same manner, FRET can also be used to elucidate drug release or polymer degradation. Thus, a real-time, on site, and quantitative monitoring can be achieved. In conclusion, the success of biodegradable fluorescent materials lies in our ability to custom design biodegradable polymers with tunable fluorescent properties to achieve appropriate physicochemical and photophysical properties to elicit favorable biological responses and meet the versatile needs in biological and biomedical applications.

## Acknowledgements

This work was supported in part by a R01 award (EB012575) from the National Institute of Biomedical Imaging and Bioengineering (NIBIB), and a National Science Foundation (NSF) CAREER award 0954109.

## References

- 1 E. S. Gil and S. M. Hudson, *Prog. Polym. Sci.*, 2004, **29**, 1173–1222.
- 2 M. Okada, *Prog. Polym. Sci.*, 2002, **27**, 87–133.
- 3 H. Y. Tian, Z. H. Tang, X. L. Zhuang, X. S. Chen and X. B. Jing, *Prog. Polym. Sci.*, 2012, **37**, 237–280.
- 4 L. S. Nair and C. T. Laurencin, *Prog. Polym. Sci.*, 2007, **32**, 762–798.
- 5 W. Amass, A. Amass and B. Tighe, *Polym. Int.*, 1998, **47**, 89–144.
- 6 N. Larson and H. Ghandehari, *Chem. Mater.*, 2012, **24**, 840–853.
- 7 Y. Ikada and H. Tsuji, *Macromol. Rapid Commun.*, 2000, **21**, 117–132.
- 8 J. Yang, A. R. Webb and G. A. Ameer, *Adv. Mater.*, 2004, **16**, 511–516.
- 9 Y. D. Wang, G. A. Ameer, B. J. Sheppard and R. Langer, *Nat. Biotechnol.*, 2002, **20**, 602–606.
- 10 S. L. He, M. J. Yaszemski, A. W. Yasko, P. S. Engel and A. G. Mikos, *Biomaterials*, 2000, **21**, 2389–2394.
- 11 X. Michalet, F. F. Pinaud, L. A. Bentolila, J. M. Tsay, S. Doose, J. J. Li, G. Sundaresan, A. M. Wu, S. S. Gambhir and S. Weiss, *Science*, 2005, **307**, 538–544.
- 12 J. O. Escobedo, O. Rusin, S. Lim and R. M. Strongin, *Curr. Opin. Chem. Biol.*, 2010, **14**, 64–70.
- 13 Y. H. Gong, Q. L. Zhou, C. Y. Gao and J. C. Shen, *Acta Biomater.*, 2007, **3**, 531–540.
- 14 E. M. Pridgen, R. Langer and O. C. Farokhzad, *Nanomedicine*, 2007, **2**, 669–680.
- 15 H. Ghandehari, *Adv. Drug Delivery Rev.*, 2008, **60**, 956.
- 16 B. Sumer and J. M. Gao, *Nanomedicine*, 2008, **3**, 137–140.
- 17 O. C. Farokhzad, A. Khademhosseini, S. Y. Yon, A. Hermann, J. J. Cheng, C. Chin, A. Kiselyuk, B. Teply, G. Eng and R. Langer, *Anal. Chem.*, 2005, **77**, 5453–5459.
- 18 V. Bagalkot, L. Zhang, E. Levy-Nissenbaum, S. Jon, P. W. Kantoff, R. Langer and O. C. Farokhzad, *Nano Lett.*, 2007, **7**, 3065–3070.
- 19 F. Wang, W. B. Tan, Y. Zhang, X. P. Fan and M. Q. Wang, *Nanotechnology*, 2006, **17**, R1–R13.
- 20 J. H. Kim, K. Park, H. Y. Nam, S. Lee, K. Kim and I. C. Kwon, *Prog. Polym. Sci.*, 2007, **32**, 1031–1053.
- 21 S. M. Janib, A. S. Moses and J. A. MacKay, *Adv. Drug Delivery Rev.*, 2010, **62**, 1052–1063.
- 22 G. S. He, L. S. Tan, Q. Zheng and P. N. Prasad, *Chem. Rev.*, 2008, **108**, 1245–1330.
- 23 A. Brenier and A. M. Jurdyc, *J. Lumin.*, 1996, **69**, 131–140.
- 24 R. K. P. Benninger, M. Hao and D. W. Piston, *Rev. Physiol., Biochem., Pharmacol.*, 2008, **160**, 71–92.
- 25 T. Kogej, D. Beljonne, F. Meyers, J. W. Perry, S. R. Marder and J. L. Bredas, *Chem. Phys. Lett.*, 1998, **298**, 1–6.
- 26 J. Smyder and T. Krauss, *Mater. Today*, 2011, **14**, 16.
- 27 L. W. K. Chung, X. H. Gao, Y. Y. Cui, R. M. Levenson and S. M. Nie, *Nat. Biotechnol.*, 2004, **22**, 969–976.
- 28 K. Rajeshwar, N. R. de Tacconi and C. R. Chenthamarakshan, *Chem. Mater.*, 2001, **13**, 2765–2782.
- 29 T. Trindade, P. O'Brien and N. L. Pickett, *Chem. Mater.*, 2001, **13**, 3843–3858.
- 30 N. Tomczak, D. Janczewski, M. Y. Han and G. J. Vancso, *Prog. Polym. Sci.*, 2009, **34**, 393–430.

- 31 A. Hirsch, Z. F. Chen and H. J. Jiao, *Angew. Chem., Int. Ed.*, 2000, **39**, 3915.
- 32 W. I. Lee, Y. J. Bae and A. J. Bard, *J. Am. Chem. Soc.*, 2004, **126**, 8358–8359.
- 33 D. Wang, T. Imae and M. Miki, *J. Colloid Interface Sci.*, 2007, **306**, 222–227.
- 34 C. C. Chu and T. Imae, *Macromol. Rapid Commun.*, 2009, **30**, 89–93.
- 35 R. Y. Tsien, *Annu. Rev. Biochem.*, 1998, **67**, 509–544.
- 36 A. B. Cubitt, R. Heim, S. R. Adams, A. E. Boyd, L. A. Gross and R. Y. Tsien, *Trends Biochem. Sci.*, 1995, **20**, 448–455.
- 37 L. A. Gross, G. S. Baird, R. C. Hoffman, K. K. Baldrige and R. Y. Tsien, *Proc. Natl. Acad. Sci. U. S. A.*, 2000, **97**, 11990–11995.
- 38 N. C. Shaner, P. A. Steinbach and R. Y. Tsien, *Nat. Methods*, 2005, **2**, 905–909.
- 39 N. C. Shaner, R. E. Campbell, P. A. Steinbach, B. N. G. Giepmans, A. E. Palmer and R. Y. Tsien, *Nat. Biotechnol.*, 2004, **22**, 1567–1572.
- 40 J. Yang, Y. Zhang, S. Gautam, L. Liu, J. Dey, W. Chen, R. P. Mason, C. A. Serrano, K. A. Schug and L. Tang, *Proc. Natl. Acad. Sci. U. S. A.*, 2009, **106**, 10086–10091.
- 41 M. Martinez-Palau, L. Urpi, X. Solans and J. Puiggali, *Acta Crystallogr., Sect. C: Cryst. Struct. Commun.*, 2006, **62**, O262–O264.
- 42 k. Knyazhanskii, P. Karmazin, P. Olekhovich and N. Dorofeenko, *J. Appl. Spectrosc.*, 1975, **23**, 3.
- 43 A. P. Demchenko, *Luminescence*, 2002, **17**, 19–42.
- 44 S. Luo, E. Zhang, Y. Su, T. Cheng and C. Shi, *Biomaterials*, 2011, **32**, 7127–7138.
- 45 A. Qin, J. W. Y. Lam and B. Z. Tang, *Prog. Polym. Sci.*, 2012, **37**, 182–209.
- 46 Y. N. Hong, J. W. Y. Lam and B. Z. Tang, *Chem. Commun.*, 2009, 4332–4353.
- 47 B. S. Gaylord, S. J. Wang, A. J. Heeger and G. C. Bazan, *J. Am. Chem. Soc.*, 2001, **123**, 6417–6418.
- 48 K. Chang and F. Jaffer, *J. Nucl. Cardiol.*, 2008, **15**, 417–428.
- 49 A. Paganin-Gioanni, E. Bellard, L. Paquereau, V. Ecochard, M. Golzio and J. Teissie, *Radiol. Oncol.*, 2010, **44**, 142–148.
- 50 A. M. Derfus, W. C. W. Chan and S. N. Bhatia, *Nano Lett.*, 2004, **4**, 11–18.
- 51 C. Kirchner, T. Liedl, S. Kudera, T. Pellegrino, A. M. Javier, H. E. Gaub, S. Stolzle, N. Fertig and W. J. Parak, *Nano Lett.*, 2005, **5**, 331–338.
- 52 D. W. Han, K. Matsumura, B. Kim and S. H. Hyon, *Bioorg. Med. Chem.*, 2008, **16**, 9652–9659.
- 53 H. S. Liu, M. S. Jan, C. K. Chou, P. H. Chen and N. J. Ke, *Biochem. Biophys. Res. Commun.*, 1999, **260**, 712–717.
- 54 A. F. E. Hezinger, J. Tessmar and A. Gopferich, *Eur. J. Pharm. Biopharm.*, 2008, **68**, 138–152.
- 55 L. Donaldson, *Mater. Today*, 2011, **14**, 131.
- 56 M. L. Schipper, G. Iyer, A. L. Koh, Z. Cheng, Y. Ebenstein, A. Aharoni, S. Keren, L. A. Bentolila, J. Q. Li, J. H. Rao, X. Y. Chen, U. Banin, A. M. Wu, R. Sinclair, S. Weiss and S. S. Gambhir, *Small*, 2009, **5**, 126–134.
- 57 W. A. Hild, M. Breunig and A. Gopferich, *Eur. J. Pharm. Biopharm.*, 2008, **68**, 153–168.
- 58 U. Resch-Genger, M. Grabolle, S. Cavaliere-Jaricot, R. Nitschke and T. Nann, *Nat. Methods*, 2008, **5**, 763–775.
- 59 M. G. Finn and V. V. Fokin, *Chem. Soc. Rev.*, 2010, **39**, 1231–1232.
- 60 J. Hong, Q. Luo, X. M. Wan, Z. S. Petrovic and B. K. Shah, *Biomacromolecules*, 2012, **13**, 261–266.
- 61 J. Rautio, H. Kumpulainen, T. Heimbach, R. Oliyai, D. Oh, T. Jarvinen and J. Savolainen, *Nat. Rev. Drug Discovery*, 2008, **7**, 255–270.
- 62 H. Zhao, B. Rubio, P. Sapra, D. C. Wu, P. Reddy, P. Sai, A. Martinez, Y. Gao, Y. Lozanguiez, C. Longley, L. M. Greenberger and I. D. Horak, *Bioconjugate Chem.*, 2008, **19**, 849–859.
- 63 M. P. Melancon, W. Wang, Y. Wang, R. Shao, X. Ji, J. G. Gelovani and C. Li, *Pharm. Res.*, 2007, **24**, 1217–1224.
- 64 Z. R. Lu, *Adv. Drug Delivery Rev.*, 2010, **62**, 246–257.
- 65 K. D. Jensen, P. Kopeckova, J. H. Bridge and J. Kopecek, *AAPS PharmSci*, 2001, **3**, E32.
- 66 F. Helmchen and W. Denk, *Nat. Methods*, 2005, **2**, 932–940.
- 67 X. Hong, W. Guo, H. Yuang, J. Li, Y. M. Liu, L. Ma, Y. B. Bai and T. J. Li, *J. Magn. Magn. Mater.*, 2004, **269**, 95–100.
- 68 D. Bhadra, S. Bhadra, S. Jain and N. K. Jain, *Int. J. Pharm.*, 2003, **257**, 111–124.
- 69 V. Sokolova, S. Neumann, A. Kovtun, S. Chernousova, R. Heumann and M. Eppele, *J. Mater. Sci.*, 2010, **45**, 4952–4957.
- 70 H. Y. Nam, K. Nam, H. J. Hahn, B. H. Kim, H. J. Lim, H. J. Kim, J. S. Choi and J. S. Park, *Biomaterials*, 2009, **30**, 665–673.
- 71 I. J. Majoros, A. Myc, T. Thomas, C. B. Mehta and J. R. Baker, Jr, *Biomacromolecules*, 2006, **7**, 572–579.
- 72 T. Imae and D. J. Wang, *J. Am. Chem. Soc.*, 2004, **126**, 13204–13205.
- 73 S. Santra and A. Malhotra, *Wiley Interdiscip. Rev.: Nanomed. Nanobiotechnol.*, 2011, DOI: 10.1002/wnan.134.
- 74 I. Brigger, C. Dubernet and P. Couvreur, *Adv. Drug Delivery Rev.*, 2002, **54**, 631–651.
- 75 Y. R. Lee, Y. H. Lee, S. A. Im, K. Kim and C. K. Lee, *Immune Netw.*, 2011, **11**, 163–168.
- 76 B. Le Droumaguet, H. Souguir, D. Brambilla, R. Verpillot, J. Nicolas, M. Taverna, P. Couvreur and K. Andrieux, *Int. J. Pharm.*, 2011, **416**, 453–460.
- 77 S. H. Kim, J. H. Jeong, K. W. Chun and T. G. Park, *Langmuir*, 2005, **21**, 8852–8857.
- 78 Y. I. Chung, J. C. Kim, Y. H. Kim, G. Tae, S. Y. Lee, K. Kim and I. C. Kwon, *J. Controlled Release*, 2010, **143**, 374–382.
- 79 P. Kocbek, N. Obermajer, M. Cegnar, J. Kos and J. Kristl, *J. Controlled Release*, 2007, **120**, 18–26.
- 80 Q. Liu, R. Li, Z. Zhu, X. Qian, W. Guan, L. Yu, M. Yang, X. Jiang and B. Liu, *Int J Pharm.*, 2012, **430**, 350–358.
- 81 T. Nam, S. Park, S. Y. Lee, K. Park, K. Choi, I. C. Song, M. H. Han, J. J. Leary, S. A. Yuk, I. C. Kwon, K. Kim and S. Y. Jeong, *Bioconjugate Chem.*, 2010, **21**, 578–582.
- 82 N. Artzi, N. Oliva, C. Puron, S. Shitreet, S. Artzi, A. bon Ramos, A. Groothuis, G. Sahagian and E. R. Edelman, *Nat. Mater.*, 2011, **10**, 704–709.



- 83 L. F. Qi and X. H. Gao, *Expert Opin. Drug Delivery*, 2008, **5**, 263–267.
- 84 M. A. Walling, J. A. Novak and J. R. Shepard, *Int. J. Mol. Sci.*, 2009, **10**, 441–491.
- 85 Y. Y. Cheng, L. B. Zhao, Y. W. Li and T. W. Xu, *Chem. Soc. Rev.*, 2011, **40**, 2673–2703.
- 86 D. J. Bharali, M. Khalil, M. Gurbuz, T. M. Simone and S. A. Mousa, *Int. J. Nanomed.*, 2009, **4**, 1–7.
- 87 D. Crouch, S. Norager, P. O'Brien, J. H. Park and N. Pickett, *Philos. Trans. R. Soc., A*, 2003, **361**, 297–310.
- 88 H. S. Choi, W. Liu, P. Misra, E. Tanaka, J. P. Zimmer, B. I. Ipe, M. G. Bawendi and J. V. Frangioni, *Nat. Biotechnol.*, 2007, **25**, 1165–1170.
- 89 Y. J. Zhang and A. Clapp, *Sensors*, 2011, **11**, 11036–11055.
- 90 X. D. Hou, Q. B. Li, L. Jia, Y. Li, Y. D. Zhu and A. M. Cao, *Macromol. Biosci.*, 2009, **9**, 551–562.
- 91 H. S. Choi, W. H. Liu, F. B. Liu, K. Nasr, P. Misra, M. G. Bawendi and J. V. Frangioni, *Nat. Nanotechnol.*, 2010, **5**, 42–47.
- 92 M. J. Murcia, D. L. Shaw, E. C. Long and C. A. Naumann, *Opt. Commun.*, 2008, **281**, 1771–1780.
- 93 B. Dubertret, P. Skourides, D. J. Norris, V. Noireaux, A. H. Brivanlou and A. Libchaber, *Science*, 2002, **298**, 1759–1762.
- 94 N. Kumar, M. N. V. Ravikumar and A. J. Domb, *Adv. Drug Delivery Rev.*, 2001, **53**, 23–44.
- 95 R. Di Corato, A. Quarta, P. Piacenza, A. Ragusa, A. Figuerola, R. Buonsanti, R. Cingolani, L. Manna and T. Pellegrino, *J. Mater. Chem.*, 2008, **18**, 1991–1996.
- 96 H. Mattoussi, G. Palui and H. B. Na, *Adv. Drug Delivery Rev.*, 2012, **64**, 138–166.
- 97 B. G. Zanetti-Ramos, E. Lemos-Senna, V. Soldi, R. Borsali, E. Cloutet and H. Cramail, *Polymer*, 2006, **47**, 8080–8087.
- 98 F. Y. Cheng, S. P. H. Wang, C. H. Su, T. L. Tsai, P. C. Wu, D. B. Shieh, J. H. Chen, P. C. H. Hsieh and C. S. Yeh, *Biomaterials*, 2008, **29**, 2104–2112.
- 99 B. J. Nehilla, P. G. Allen and T. A. Desai, *ACS Nano*, 2008, **2**, 538–544.
- 100 J. S. Kim, K. J. Cho, T. H. Tran, M. Nurunnabi, T. H. Moon, S. M. Hong and Y. K. Lee, *J. Colloid Interface Sci.*, 2011, **353**, 363–371.
- 101 B. Y. S. Kim, W. Jiang, J. Oreopoulos, C. M. Yip, J. T. Rutka and W. C. W. Chan, *Nano Lett.*, 2008, **8**, 3887–3892.
- 102 J. Cao, H. Y. Zhu, D. W. Deng, B. Xue, L. P. Tang, D. Mahounga, Z. Y. Qian and Y. Q. Gu, *J. Biomed. Mater. Res., Part A*, 2012, **100**, 958–968.
- 103 Y. L. Xu, L. Q. Shi, R. J. Ma, W. Q. Zhang, Y. L. An and X. X. Zhu, *Polymer*, 2007, **48**, 1711–1717.
- 104 Y. J. Gong, M. Y. Gao, D. Y. Wang and H. Mohwald, *Chem. Mater.*, 2005, **17**, 2648–2653.
- 105 C. L. Wu, R. J. Ma, H. He, L. Z. Zhao, H. J. Gao, Y. L. An and L. Q. Shi, *Macromol. Biosci.*, 2009, **9**, 1185–1193.
- 106 J. M. Tavares, L. M. Fletcher and G. I. Welsh, *J. Endocrinol.*, 2001, **170**, 297–306.
- 107 D. M. Chudakov, M. V. Matz, S. Lukyanov and K. A. Lukyanov, *Physiol. Rev.*, 2010, **90**, 1103–1163.
- 108 D. W. Piston and G. J. Kremers, *Trends Biochem. Sci.*, 2007, **32**, 407–414.
- 109 A. Miyawaki, J. Llopis, R. Heim, J. M. McCaffery, J. A. Adams, M. Ikura and R. Y. Tsien, *Nature*, 1997, **388**, 882–887.
- 110 Y. Kang, J. Yang, S. Khan, L. Anissian and G. A. Ameer, *J. Biomed. Mater. Res., Part A*, 2006, **77**, 331–339.
- 111 R. Y. Tsien, *Angew. Chem., Int. Ed.*, 2009, **48**, 5612–5626.